Optimal Operation of Soft Open Points in Active Distribution Networks Under Three-Phase Unbalanced Conditions

Peng Li, *Member, IEEE*, Haoran Ji, *Student Member, IEEE*, Chengshan Wang, *Senior Member, IEEE*, Jinli Zhao, *Member, IEEE*, Guanyu Song, Fei Ding, *Member, IEEE*, and Jianzhong Wu, *Member, IEEE*

***Abstract*—The asymmetric integration of distributed generators (DGs) exacerbates the three-phase unbalanced condition in distribution systems. The serious unbalanced operation causes inefficient utilization of network assets and security risks in the system. Soft open point (SOP) is a flexible power electronic device which can achieve accurate active and reactive power flow control to balance the power flow among phases. This paper proposes an SOPs-based operation strategy for unbalanced active distribution networks. By regulating the operation of SOPs, the strategy can reduce power losses and simultaneously mitigate the three-phase unbalance of the upper-level grid. Semidefinite programming (SDP) relaxation is advocated to convert the original non-convex, nonlinear optimization model into an SDP formulation, which can be efficiently solved to meet the requirement of rapid adjustment. Case studies are conducted on the modified IEEE 33-node and IEEE 123-node distribution system to verify the effectiveness and efficiency of the proposed strategy.**

***Index Terms*—Active distribution network, distributed generator (DG), soft open point (SOP), unbalanced operation, semidefinite programming.**

NOMENCLATURE

Sets

Ω_{b}	Set of all branches
Ω_{n}	Set of all nodes
Φ_i	Set of phases for node i, $\Phi_i \subseteq \{a, b, c\}$
Φ_{ij}	Set of phases for branch ij, $\Phi_{ij} \subseteq \{a, b, c\}$.

Indices

i, j	Indices of nodes, from 1 to N_{N}
φ	Indices of phases, referring to a, b and c.

Variables

$V_{\varphi,i}, V_i$	Complex voltage on phase φ of node i, defined as $V_i := (V_{\varphi,i}, \varphi \in \Phi_i) \in \mathbb{C}^{\lvert\Phi_i\rvert}$
$I_{\varphi,ij}, I_{ij}$	Complex current on phase φ of branch ij, defined as $I_{ij} := (I_{\varphi,ij}, \varphi \in \Phi_{ij}) \in \mathbb{C}^{\lvert\Phi_{ij}\rvert}$
$s_{\varphi,i}, s_i$	Complex power injection on phase φ of node i, defined as $s_i := (s_{\varphi,i}, \varphi \in \Phi_{ij}) \in \mathbb{C}^{\lvert\Phi_i\rvert}$
v_i, l_{ij}	Auxiliary variables that indicate $v_i := V_i V_i^{\mathrm{H}} \in \mathbb{C}^{\lvert\Phi_i\rvert\times\lvert\Phi_i\rvert}$, and $l_{ij} := I_{ij} I_{ij}^{\mathrm{H}} \in \mathbb{C}^{\lvert\Phi_{ij}\rvert\times\lvert\Phi_{ij}\rvert}$
S_{ij}	Complex power flow of branch ij, defined as $S_{ij} = V_i I_{ij}^{\mathrm{H}}$
$P_{\varphi,i}^{\mathrm{DG}}, Q_{\varphi,i}^{\mathrm{DG}}$	Active/reactive power injection by DG on phase φ at node i
$P_{\varphi,i}^{\mathrm{SOP}}, Q_{\varphi,i}^{\mathrm{SOP}}$	Active/reactive power injection by SOP on phase φ at node i
$P_{\varphi,i}^{\mathrm{SOP,loss}}$	Active power losses of SOP on phase φ at node i
$V_{i,+}, V_{i,-}$	Positive/negative sequence voltage at node i.

Parameters

N_{N}	Total number of nodes
$P_{\varphi,i}^{\mathrm{L}}, Q_{\varphi,i}^{\mathrm{L}}$	Active/reactive power consumption on phase φ at node i
$P_{\varphi,i}^{\mathrm{DG,re}}$	Given active power generated by DG on phase φ at node i
$\tan\theta_{\varphi,i}^{\mathrm{DG}}$	$\cos\theta_{\varphi,i}^{\mathrm{DG}}$ is the power factor of DG on phase φ at node i
$S_{\varphi,i}^{\mathrm{DG}}$	Capacity limit of DGconnected to node i on phase φ
$\overline{Q}_{\varphi,i}^{\mathrm{SOP}}, \underline{Q}_{\varphi,i}^{\mathrm{SOP}}$	Upper/lower limit of reactive power provided by SOP on phase φ at node i
$S_{\varphi,i}^{\mathrm{SOP}}$	Capacity limit of SOPconnected to node i on phase φ
z_{ij}	Impedance matrix of branch ij
$\overline{V}_i, \underline{V}_i$	Upper/lower voltage limit of node i
$\overline{L}_{ij}$	Upper current limit of branch ij
A_i^{SOP}	Loss coefficient of SOP at node i
$W_\alpha, W_\beta, W_\gamma$	Weight coefficients associated with each term in objective function.

Manuscript received January 6, 2017; revised April 26, 2017 and July 9, 2017; accepted August 9, 2017. Date of publication August 15, 2017; date of current version December 19, 2018. This work was supported in part by the National Key Technology Research and Development Program of China under Grant 2016YFB0900105, and in part by the National Natural Science Foundation of China under Grant 51261130473. Paper no. TSG-00028-2017. *(Corresponding author: Chengshan Wang.)*

P. Li, H. Ji, C. Wang, J. Zhao, and G. Song are with the Key Laboratory of Smart Grid of Ministry of Education, Tianjin University, Tianjin 300072, China (e-mail: lip@tju.edu.cn; jihaoran@tju.edu.cn; cswang@tju.edu.cn).

F. Ding is with National Renewable Energy Laboratory, Golden, CO 80214 USA (e-mail: fei.ding@nrel.gov).

J. Wu is with the Institute of Energy, School of Engineering, Cardiff University, Cardiff CF24 3AA, U.K. (e-mail: wuj5@cardiff.ac.uk).

Color versions of one or more of the figures in this paper are available online at http://ieeexplore.ieee.org.

Digital Object Identifier 10.1109/TSG.2017.2739999

I. INTRODUCTION

DISTRIBUTED generators (DGs) including intermittent renewable energy resources have increasingly been integrated into distribution networks recently [1]. Distribution networks are gradually being transformed from passive networks into active distribution networks (ADNs) comprising the roles of energy collection, transmission, storage and distribution [2], [3]. Highly volatile DGs participate in the operation of ADNs, making operation relatively complex and challenging [4], [5].

Distribution networks are usually unbalanced due to the asymmetric three-phase line configuration and a large number of single-phase loads. The asymmetric access of DGs with high penetration further exacerbates the unbalanced condition [6]. The unbalanced operation of ADNs will increase the operational losses [7] and cause inefficient utilization of network assets by reducing the available capacity [8], [9]. Negative sequence components decomposed by unbalanced voltages may also result in distribution equipment operating in an abnormal condition [10]. Most existing approaches simplify the three-phase distribution network as a balanced system using a single-phase equivalent model for calculations. However, it is inconsistent with reality at the low-voltage level, and the calculation results will deviate from the practical state of ADNs. It is indispensable to mitigate the unbalanced condition and optimize the operation of ADNs by adopting a three-phase model.

In current ADNs, the regulation ability of the primary equipment has become the main bottleneck restricting improvement of the operating level. Conventional three-phase balancing is conducted primarily by network reconfiguration [11] and re-phasing strategies for laterals and distribution transformers [12]. Limited by slow response and discrete adjustment due to switching, conventional balancing strategies based on primary equipment have difficulty meeting the requirement of rapid operation with high precision when DGs and loads fluctuate frequently in ADNs [13]. The development of power electronic technologies provides opportunities for further optimization of ADN operation. Soft open point (SOP) [14] is a highly controllable power electronic device installed to replace a normally open point (NOP), for a flexible connection between feeders in distribution networks. Compared to conventional switching operation, an SOP can accurately realize three-phase power flow control and provide the reactive power support [15]. Thus, it is significant to study the operating strategies of SOPs for unbalanced ADNs.

Previous studies have investigated the three-phase optimal operation problems of unbalanced ADNs. Reference [16] proposed an optimization method based on three-phase current injection, involving DGs and VAR regulation strategies to minimize the negative sequence voltage of the system. Mostafa *et al.* [17] developed a genetic algorithm to minimize phase unbalance and power losses in a three-phase unbalanced distribution system with single-phase photovoltaics (PVs). The models presented in [16] and [17] essentially all derived using nonconvex nonlinear programming (NLP) which cannot guarantee global optimality of their solutions in most cases. In [18], a three-phase VAR optimization model was developed to minimize power losses of unbalanced ADNs based on the second-order cone relaxation method, which improved computation efficiency substantially. The coupling between phases and unbalanced condition mitigation could be further considered in this model. Reference [19] developed a method to optimally regulate bus voltages for unbalanced distribution systems via a convex quadratic optimization programming. Wang *et al.* [20] proposed a three-phase microgrid restoration model considering unbalanced operation of DGs, with a quadratic objective function and linearized constraints. Reference [21] first proposed a bus injection model to solve the optimal power flow problem through semidefinite programming (SDP) relaxation for radial networks. Robbins *et al*. [22] extended the SDP-based optimal power flow approach to optimally set the tap position of voltage regulation transformers in unbalanced distribution networks. Dall'Anese *et al.* [23] developed an SDP relaxation to solve the OPF problem for microgrids operating in an unbalanced case. The virtues of the SDP relaxation in the case of the optimal dispatch of photovoltaic inverters were further demonstrated in [24]. It was shown in [25] and [26] that SOPs significantly facilitated the economic operation of ADNs by optimizing active power flow and providing reactive power support. The studies in [25] and [26] both assumed that the three-phase distribution networks are balanced, and they could be extended to the optimal operation of unbalanced ADNs.

Considering the asymmetric access of DGs with high penetration, the unbalanced condition of ADNs is severe. SOPs can rapidly regulate the three-phase active and reactive power flow to mitigate unbalances and reduce operational losses of ADNs. Enclosed by the AC power flow equations and operation constraints of SOPs, the proposed unbalanced operation problems based on SOPs are highly non-convex NLP problems. The non-convexity and nonlinearity result in the proposed NLP problems generally being non-deterministic polynomial-time hard (NP-hard) to solve [27], [28], meaning that these problems require solution times that scale exponentially with problem size. In addition, as NLP problems only can guarantee locally optimal solutions, obtaining the global solution of large-scale NLP problems in reasonable computational times is a major challenge [28]. And it puts forward higher requirements for accuracy and efficiency of the solving method. With an exact convex relaxation, the problem of NP-hardness is largely avoided and the global optimum can be obtained [29].

This paper proposes an optimal operation strategy for unbalanced ADNs based on SOPs, mitigating the three-phase unbalances while enhancing the operational efficiency of ADNs. The main contributions are summarized as follows:

1) The potential benefits of SOPs for unbalanced ADNs operation are fully explored. An SOP-based optimal operation strategy for unbalanced ADNs is proposed. The strategy optimizes the regulation of SOPs to mitigate the three-phase unbalanced condition while minimizing power losses simultaneously.
2) SDP relaxation is adopted to convert the original non-convex nonlinear optimization model into an SDP formulation, which can be efficiently solved to meet the demands of rapid centralized control.

The remainder of this paper is organized as follows. Section II builds the three-phase operation optimization model for unbalanced ADNs based on SOPs. The original problem

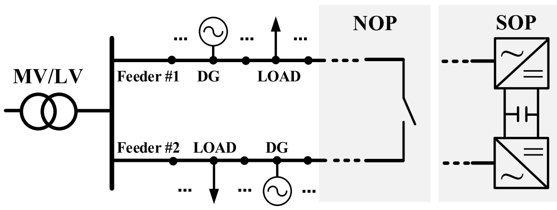

Fig. 1. Schematic of SOP installation.

is converted into an SDP model using convex relaxation in Section III. Case studies are given in Section IV to verify the effectiveness of the proposed strategy using two modified IEEE test systems. Section V concludes the paper with a discussion.

II. Three-Phase Optimal Operation Problem Formulation Based on SOPs

Considering the reduction of power losses and the mitigation of unbalanced condition simultaneously, an SOPs-based operation strategy is developed in this section. By regulating the operation of SOPs in ADNs, the strategy can effectively achieve the both goals.

A. Principle and Modeling of SOP

An SOP is installed between adjacent feeders to replace the NOP in ADNs [14], as shown in Fig. 1. Compared to traditional switch operation, SOPs can precisely control the power flow with lower operational costs and avoid the risk caused by frequent switching actions, which significantly improves the control flexibility and rapidity of ADNs.

The implementation of an SOP is based on power electronic devices, which usually employs back-to-back voltage source converters (B2B VSCs). B2B VSCs can accurately adjust the power flow between the connected feeders in real-time, and provide voltage and reactive power support to increase the flexibility of ADN operation [30].

The controllable variables for SOPs consist of the three-phase active and reactive power outputs of two converters. The three-phase powers of SOPs can be controlled independently, assuming the three-phase SOP consists of three single-phase SOP modules. Although the efficiency of B2B VSC is sufficiently high, it inevitably produces losses when large-scale power transfer occurs. The reactive power outputs of two converters are independent of each other because of DC isolation, and each is only required to meet its own capacity constraint. PQ-V_{dc}Q is commonly selected as the control mode under normal conditions, indicating that one converter controls its active/reactive power output, the other controls its reactive power output and simultaneously maintains a constant DC-side voltage. The optimization model of an SOP is obtained, with the following constraints.

1) SOP Active Power Constraints:

$$P_{\varphi,i}^{\mathrm{SOP}} + P_{\varphi,j}^{\mathrm{SOP}} + P_{\varphi,i}^{\mathrm{SOP,loss}} + P_{\varphi,j}^{\mathrm{SOP,loss}} = 0 \tag{1}$$

$$P_{\varphi,i}^{\mathrm{SOP,loss}} = A_i^{\mathrm{SOP}} \sqrt{\left(P_{\varphi,i}^{\mathrm{SOP}}\right)^2 + \left(Q_{\varphi,i}^{\mathrm{SOP}}\right)^2} \tag{2}$$

$$P_{\varphi,j}^{\mathrm{SOP,loss}} = A_j^{\mathrm{SOP}} \sqrt{\left(P_{\varphi,j}^{\mathrm{SOP}}\right)^2 + \left(Q_{\varphi,j}^{\mathrm{SOP}}\right)^2}. \tag{3}$$

2) SOP Reactive Power Constraints:

$$\underline{Q}_{\varphi,i}^{\mathrm{SOP}} \le Q_{\varphi,i}^{\mathrm{SOP}} \le \overline{Q}_{\varphi,i}^{\mathrm{SOP}} \tag{4}$$

$$\underline{Q}_{\varphi,j}^{\mathrm{SOP}} \le Q_{\varphi,j}^{\mathrm{SOP}} \le \overline{Q}_{\varphi,j}^{\mathrm{SOP}}. \tag{5}$$

3) SOP Capacity Constraints:

$$\sqrt{\left(P_{\varphi,i}^{\mathrm{SOP}}\right)^2 + \left(Q_{\varphi,i}^{\mathrm{SOP}}\right)^2} \le S_{\varphi,i}^{\mathrm{SOP}} \tag{6}$$

$$\sqrt{\left(P_{\varphi,j}^{\mathrm{SOP}}\right)^2 + \left(Q_{\varphi,j}^{\mathrm{SOP}}\right)^2} \le S_{\varphi,j}^{\mathrm{SOP}}. \tag{7}$$

B. Modeling of Unbalanced Operation Problem of ADNs Based on SOPs

1) Objective Function: The optimal operation of unbalanced ADNs mainly focuses on the mitigation of unbalanced conditions. Araujo *et al.* [31] minimize the voltage unbalance by the summation of the negative sequence system voltages. Reference [17] further proposed a multi-objective strategy to minimize the current unbalance of the whole distribution system. Minimizing the power losses is also widely adopted for the operation of unbalanced ADNs [16], [17]. This paper considers the operational efficiency and unbalanced condition of ADNs simultaneously, and proposes a linear weighted combination of minimum total power losses, the voltage unbalanced condition and the current unbalanced condition of the substation as the objective function, which is formulated as follows.

$$\min f = W_\alpha f^{\mathrm{loss}} + W_\beta f^{\mathrm{V}} + W_\gamma f^{\mathrm{I}} \tag{8}$$

where the power losses f^{loss}, the voltage unbalanced condition f^{V} and the current unbalanced condition of the substation f^{I} are formulated as follows:

$$f^{\mathrm{loss}} = \sum_{i=1}^{N_{\mathrm{N}}} \sum_{\varphi=a}^{c} \mathrm{Re}\left(s_{\varphi,i}\right) \tag{9}$$

$$f^{\mathrm{V}} = \sum_{i=1}^{N_{\mathrm{N}}} \sum_{\varphi=a}^{c} \left| V_{\varphi,i} - \frac{1}{3}\left(V_{a,i} + V_{b,i} + V_{c,i}\right) \right| \tag{10}$$

$$f^{\mathrm{I}} = \sum_{\varphi=a}^{c} \left| I_{\varphi,0} - \frac{1}{3}\left(I_{a,0} + I_{b,0} + I_{c,0}\right) \right| \tag{11}$$

where $I_{\varphi,0}$ denotes the complex current on phase φ of the substation outlet. The overall active power losses f^{loss} include the network losses and the power losses caused by the power transmission of SOPs.

The weighted sum method (WSM) [32] is applied to the above multi-objective optimization problem. The weight coefficients W_α, W_β, and W_γ of each term in (8) can be determined by analytic hierarchy process (AHP) [33] according to the experience of the distribution system operators (DSOs). In addition, the coefficients satisfy $W_\alpha + W_\beta + W_\gamma = 1.0$.

The constraints include the operation constraints of distribution networks and the operation constraints of the regulating equipment, as described below.

2) Three-Phase System Operation Constraints: The branch flow model, which is proposed for the distribution networks in [34], is adopted to model the three-phase unbalanced distribution network [35]. It can be described mathematically with the following constraints:

$$\sum_{ji\in\Omega_b}\operatorname{diag}\left(S_{ji}-z_{ji}l_{ji}\right)+s_i=\sum_{ik\in\Omega_b}\operatorname{diag}(P_i(S_{ik})) \tag{12}$$

$$P_j(v_i)-v_j-\left(S_{ij}z_{ij}^{\mathrm{H}}+z_{ij}S_{ij}^{\mathrm{H}}\right)+z_{ij}l_{ij}z_{ij}^{\mathrm{H}}=0 \tag{13}$$

$$s_{\varphi,i}=p_{\varphi,i}+\mathrm{j}q_{\varphi,i}=\left(P_{\varphi,i}^{\mathrm{DG}}+\mathrm{j}Q_{\varphi,i}^{\mathrm{DG}}\right)+\left(P_{\varphi,i}^{\mathrm{SOP}}+\mathrm{j}Q_{\varphi,i}^{\mathrm{SOP}}\right)-\left(P_{\varphi,i}^{\mathrm{L}}+jQ_{\varphi,i}^{\mathrm{L}}\right) \tag{14}$$

$$\begin{bmatrix} v_i & S_{ij} \\ S_{ij}^{\mathrm{H}} & l_{ij}\end{bmatrix}\geq 0 \tag{15}$$

$$\operatorname{rank}\begin{bmatrix} v_i & S_{ij} \\ S_{ij}^{\mathrm{H}} & l_{ij}\end{bmatrix}=1 \tag{16}$$

where $P_i(S_{ik})$ denotes lifting S_{ik} onto the set of phases Φ_i of node i with a missing phase filled with 0 and $P_j(v_i)$ denotes projecting v_i onto the set of phases Φ_j of node j.

Constraint (12) represents the complex power balance of node i. Ohm's law over branch ij is expressed as (13). The active power injection $p_{\varphi,i}$ and reactive power injection $q_{\varphi,i}$ on phase φ of node i can be described as (14). Constraints (15) and (16) indicate the semidefinite constraint and the rank-one constraint of the matrix variable for branch ij. Namely as for each branch $i\to j$, it satisfies that $S_{ij}=V_iI_{ij}^{\mathrm{H}}$ [35], which is an essential part of power flow.

The operation constraints of ADNs are expressed as follows:

$$\left(\underline{V_i}\right)^2\leq\operatorname{diag}(v_i)\leq\left(\overline{V_i}\right)^2 \tag{17}$$

$$0\leq\operatorname{diag}\left(l_{ij}\right)\leq\left(\overline{L}_{ij}\right)^2 \tag{18}$$

$$v_0=V_0^{\mathrm{ref}}\left(V_0^{\mathrm{ref}}\right)^{\mathrm{H}} \tag{19}$$

Constraint (17) denotes the upper/lower voltage limits of node i. The maximum line current capacity of branch ij is formulated as (18). V_0^{ref} represents the voltage at substation node, which is assumed as 1.0 p.u., and the angle difference between the three-phase voltage is 120 degrees.

3) DG Operation Constraints:

$$P_{\varphi,i}^{\mathrm{DG}}=P_{\varphi,i}^{\mathrm{DG,re}} \tag{20}$$

$$Q_{\varphi,i}^{\mathrm{DG}}=P_{\varphi,i}^{\mathrm{DG}}\tan\theta_{\varphi,i}^{\mathrm{DG}} \tag{21}$$

$$\sqrt{\left(P_{\varphi,i}^{\mathrm{DG}}\right)^2+\left(Q_{\varphi,i}^{\mathrm{DG}}\right)^2}\leq S_{\varphi,i}^{\mathrm{DG}} \tag{22}$$

Constraint (20) assumes that the active power generated by DGs is equal to the given value. Constraint (21) denotes the reactive power constraint of DGs and the capacity constraint of DGs is expressed as (22).

The above SOP-based optimal operation model for unbalanced ADNs is shown as (23). The decision variables in this model involve the three-phase transmitted active power and reactive power outputs of SOPs. The node voltage V_i and branch currents L_{ij} can be uniquely determined by the above unbalanced model in distribution networks [36].

$$\begin{aligned}\min\ & f=W_\alpha f^{\mathrm{loss}}+W_\beta f^{\mathrm{V}}+W_\gamma f^{\mathrm{I}}\\ \text{s.t.}\ & (1)-(7),(9)-(22)\end{aligned} \tag{23}$$

In the optimization model, $P_{\varphi,i}^{\mathrm{L}}$ and $Q_{\varphi,i}^{\mathrm{L}}$ denote the active and reactive power consumed by a wye-connected load on phase φ at node i. Thus, both single- and two- phase loads (if any) can be accommodated in the formulated model.

As a consequence, the proposed model is essentially an NLP problem, requiring to be solved accurately and efficiently.

III. SDP Model Conversion

As SOPs are directly dispatched by DSO in a centralized manner, it puts forward a strict requirement on the performance of problem solving when DGs and loads fluctuate rapidly in spatial and temporal distribution. In this section, SDP relaxation is adopted to convert the original NLP model to an SDP model, enabling rapid and accurate calculation.

A. Standard Form of Semidefinite Programming

SDP can be mathematically characterized as a type of convex programming, which can be regarded as the generalization of both linear and nonlinear programming. As SDP offers excellent performance in terms of global optimality and computational efficiency, it has been widely used in solving NLP problems. The standard form can be written as [37]:

$$\min\{\langle \boldsymbol{C},\boldsymbol{X}\rangle\,|\,\langle \boldsymbol{A_i},\boldsymbol{X}\rangle=\boldsymbol{b_i},\boldsymbol{X}\in\mathbb{S}_+\} \tag{24}$$

where $\boldsymbol{X}$ is the matrix variable. $\boldsymbol{A}$, $\boldsymbol{C}$ and $\boldsymbol{b}$ represent two constant matrices and a constant vector, respectively. $\mathbb{S}_+$ denotes the sets of Hermitian matrix. Let $\langle \boldsymbol{C},\boldsymbol{X}\rangle$ indicate the trace of the matrix product $\boldsymbol{CX}$.

As shown above, SDP has strict demands for the mathematical formulation. The objective function is a linear function of the symmetric matrix variable $\boldsymbol{X}$; its feasible region is composed of linear constraints on the elements of $\boldsymbol{X}$ and the additional constraint that $\boldsymbol{X}$ must be positive semidefinite. Therefore, the original nonconvex NLP model must be converted in advance before applying SDP.

B. Conversion to the SDP Model

Enclosed by the AC power flow equations and operation constraints of SOPs, the proposed unbalanced operation model (23) is a highly non-convex NLP problem. As rank-one constraint in (16) is the main source of non-convexity in the original model, the rank-one constraint is removed for semidefinite relaxation. The following is the reformulation of other nonlinear constraints.

The capacity constraints of SOPs in (6)–(7) and DGs in (22) can be reformulated as the following general form:

$$\sqrt{\left(P_{\varphi,i}^{\mathrm{a}}\right)^2+\left(Q_{\varphi,i}^{\mathrm{a}}\right)^2}\leq S_{\varphi,i}^{\mathrm{a}},\ \mathrm{a}\in\{\mathrm{SOP},\mathrm{DG}\} \tag{25}$$

Constraint (25) is a convex quadratic constraint, which is a special case of SDP, and it can be expressed as the following SDP form:

$$\begin{bmatrix} S^{\mathrm{a}}_{\varphi,i} & P^{\mathrm{a}}_{\varphi,i}+\mathrm{j}Q^{\mathrm{a}}_{\varphi,i} \\ P^{\mathrm{a}}_{\varphi,i}-\mathrm{j}Q^{\mathrm{a}}_{\varphi,i} & S^{\mathrm{a}}_{\varphi,i} \end{bmatrix} \succeq 0, \mathrm{a} \in \{\mathrm{SOP}, \mathrm{DG}\} \quad (26)$$

Similarly, the operation constraints of SOP in (2)–(3) can also be reformulated as the SDP form:

$$\begin{bmatrix} P^{\mathrm{SOP,loss}}_{\varphi,i}/A^{\mathrm{SOP}}_{i} & P^{\mathrm{SOP}}_{\varphi,i}+\mathrm{j}Q^{\mathrm{SOP}}_{\varphi,i} \\ P^{\mathrm{SOP}}_{\varphi,i}-\mathrm{j}Q^{\mathrm{SOP}}_{\varphi,i} & P^{\mathrm{SOP,loss}}_{\varphi,i}/A^{\mathrm{SOP}}_{i} \end{bmatrix} \succeq 0 \quad (27)$$

$$\begin{bmatrix} P^{\mathrm{SOP,loss}}_{\varphi,j}/A^{\mathrm{SOP}}_{j} & P^{\mathrm{SOP}}_{\varphi,j}+\mathrm{j}Q^{\mathrm{SOP}}_{\varphi,j} \\ P^{\mathrm{SOP}}_{\varphi,j}-\mathrm{j}Q^{\mathrm{SOP}}_{\varphi,j} & P^{\mathrm{SOP,loss}}_{\varphi,j}/A^{\mathrm{SOP}}_{j} \end{bmatrix} \succeq 0 \quad (28)$$

The absolute values of objective terms in constraints (10) and (11) are convex and can be effectively solved [38].

The main motivation of convexification for the problem is to align with the standard SDP formulation, which can be efficiently solved.

Thus, the relaxed SDP model is obtained as (29):

$$\begin{aligned} &\min\ f = W_\alpha f^{\mathrm{loss}} + W_\beta f^{\mathrm{V}} + W_\gamma f^{\mathrm{I}} \\ &\mathrm{s.t.}\ \begin{cases} (1), (4), (5), (9)-(11), (12)-(15), \\ (17)-(19), (20)-(21), (26)-(28). \end{cases} \end{aligned} \quad (29)$$

Remark 1: For medium or high voltage distribution system, single-phase equivalent model is used for the calculation and optimization of the balanced networks. Branch flow model can be used and formulated as an SOCP model, or an SDP model [28]. However, as distribution networks are inherently unbalanced due to the asymmetric lines and loads configuration, a three-phase network model is thus well motivated. Considering the SOCP-based formulation can be solved more efficiently, it is prone to convert the three-phase optimization model into an SOCP model. As SOCP relaxation eliminates the voltage and current angles, the three-phase distribution networks are independently modeled as three single-phase models in SOCP formulation [18].

To further consider the phase-to-phase coupling effects, the original model has been converted into an SDP model, in which the mutual impedance between phases of each line is not equal to zero. Thus, the proposed SDP model reflects the phase-to-phase coupling effects of line configuration, accounting for a more accurate model of the unbalanced ADNs. Specially, the SOCP relaxation is dominated by the SDP relaxation [39], as the second-order cone can be embedded in the cone of semidefinite matrices. The virtues of the SDP relaxation in the case of an unbalanced system are further demonstrated in [23].

C. Discussion of SDP Relaxation Exactness

The convex relaxation SDP model (29) provides a lower bound for the original NLP problem (23) because the original feasible set is enlarged. If the optimal solution of the SDP model satisfies the rank-one constraint (16), the solution is also optimal for the original NLP problem, and the semidefinite relaxation is exact. But as the SDP model (29) is a relaxed formulation of the original model (23), the solution could have the possibility with the rank larger than one. In such a case, the feasible rank-one approximation of the solution obtained by rank reduction techniques is generally suboptimal [29]. For balanced distribution networks, [40] has proved the conditions under which a rank-one solution is attainable if the original NLP problem is feasible. However, for unbalanced distribution networks the conclusion of [40] may no longer be effective.

An analytical characterization of the feasibility region for unbalanced cases is challenging because of the coupling of line parameters and voltage angles involved. An argument was provided in [23] to explain why a rank-one solution is expected from the relaxed SDP model even in unbalanced cases. If the original model has feasible solutions and optimization objective function is increasing with the system injected powers, the theorems of [23] show that a rank-one solution can be obtained from the relaxed SDP model.

Even though counterexamples exist where SDP relaxation is not exact for unbalanced distribution networks when the reduction of power losses is given much less importance in the objective function, numerical tests demonstrate that SDP relaxation tends to attain the optimal solution of the original nonconvex problem in many cases. For example, it is shown empirically in [34] that the relaxation is exact for all the tested distribution networks, including IEEE test feeders and practical systems. However, sufficient conditions that guarantee exact relaxation for unbalanced networks remain elusive.

To evaluate the exactness of SDP relaxation in the proposed strategy, namely, how close the matrix variable in (16) is to rank one, the largest two eigenvalues λ_1 and $\lambda_2(|\lambda_1| \geq |\lambda_2| \geq 0)$ of the matrix in (15) are computed, and its ratio $|\lambda_2/\lambda_1|$ is obtained. The smaller ratio indicates that the matrix is closer to rank one [35]. If the ratio value is sufficiently small, the SDP relaxation can be regarded as numerically exact. Otherwise, it needs to be strengthened by adding valid inequalities to the SDP model or increasingly tightening the bound of variables [40], [41].

The above SDP formulation for branch flow model is numerically more stable than the SDP formulation for bus injection model [43], [44], because it avoids the ill-conditioned matrix variables caused by subtractions of the node voltages which are very close in value in ADNs.

In summary, compared to the original NLP model, the relaxed SDP model can efficiently solve the SOPs-based optimization problem of unbalanced ADNs with acceptable accuracy for the studied cases.

IV. Case Studies and Analysis

In this section, the modified IEEE 33-node and IEEE 123-node distribution system are used to demonstrate the effectiveness and efficiency of the unbalanced optimal operation strategy based on SOPs. First, the performance of the proposed strategy involving the unbalanced condition mitigation and power loss reduction of the ADNs is analyzed on the modified IEEE 33-node system. Then, the test cases are carried out on the IEEE 123-node system to verify the scalability of the proposed method on the severe unbalanced conditions. Through comparison with a primal-dual interior point

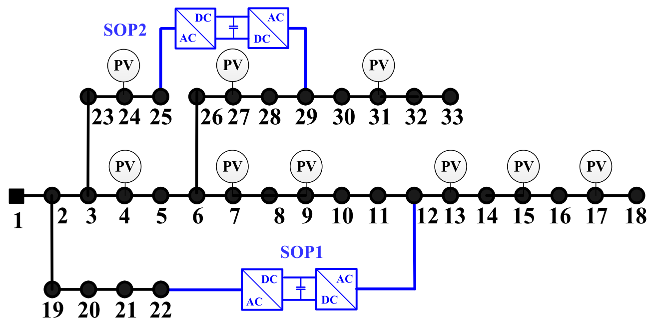

Fig. 2. Structure of the modified IEEE 33-node system.

TABLE I
BASIC INSTALLATION PARAMETERS OF PVS

Parameter	PV cells								
Location	4	7	9	13	15	17	24	27	31
Phase	A	C	B	A	B	C	B	C	A
Capacity (kVA)	200	200	200	200	300	300	200	300	300

method (IPM), the computation efficiency of the operation strategy based on SDP is verified.

The proposed strategy was implemented in the YALMIP optimization toolbox [45] with MATLAB R2013a, and solved by MOSEK 7.1.0.14. The numerical experiments were conducted on a computer with an Intel Xeon CPU E5-1620 running at 3.70 GHz with 32 GB of RAM.

A. Modified IEEE 33-Node System

As shown in Fig. 2, the test system is a modified IEEE 33-node distribution system [34], of which the unbalanced branch and load data were from [18]. The total real and reactive power loads on the system were 3635 kW and 2265 kvar, respectively.

To fully consider the impact of asymmetric access of DGs with high penetration on ADNs, nine PVs are integrated into the network with a constant power factor 1.0. The parameters are shown in Table I.

Two groups of SOP are installed between nodes 12 and 22, and between nodes 25 and 29, of which the maximum capacity on each phase is 500 kVA. It is assumed that the loss coefficient of an SOP is 0.02. The minimum and maximum allowable system voltages are set as 0.95 p.u. and 1.05 p.u., respectively.

The scaled weight coefficients in the objective function, obtained by the pairwise comparison in AHP [46] shown in Table II, are given as follows: $W_\alpha = 0.68$, $W_\beta = 0.20$, and $W_\gamma = 0.12$. Considering that the operational efficiency is an important concern for ADNs, a relatively large weight coefficient W_α has been assigned.

The voltage unbalanced condition at each node is evaluated by using the unbalance index (UI) [47], shown as follows.

$$\lambda_{\mathrm{UI},i} = \frac{|V_{i,-}|}{|V_{i,+}|} \tag{30}$$

TABLE II
PAIRWISE COMPARISONS OF THE OBJECTIVE TERMS

-	Voltage unbalanced condition	Current unbalanced condition	Power losses
Voltage unbalanced condition	1	1/2	1/5
Current unbalanced condition	2	1	1/4
Power losses	5	4	1

TABLE III
OPTIMIZATION RESULTS OF SCENARIO I AND II

Scenario	Power losses (kW)	Reduction rate of losses (%)	$\lambda_{\mathrm{UI,sys}}$	Reduction rate of $\lambda_{\mathrm{UI,sys}}$ (%)	Three-phase current of substation outlet (A)
I	93.84	-	0.0015	-	125.70/130.47/125.47
II	31.92	65.98	0.0005	66.67	71.88/71.88/71.88

The positive and negative sequence voltages $V_{i,+}$ and $V_{i,-}$ at node i can be calculated by the three-phase voltages, which are given in (31) and (32).

$$V_{i,-} = \frac{1}{3}\left(V_{a,i} + \alpha^2 V_{b,i} + \alpha V_{c,i}\right) \tag{31}$$

$$V_{i,+} = \frac{1}{3}\left(V_{a,i} + \alpha V_{b,i} + \alpha^2 V_{c,i}\right) \tag{32}$$

where angle shift $\alpha = e^{\mathrm{j}120^\circ}$.

To evaluate the overall system voltage unbalanced condition, the system UI is introduced as follows [28]:

$$\lambda_{\mathrm{UI,sys}} = \sum_{i \in \Omega_{\mathrm{n}}} \left(\frac{|V_{i,-}|^2}{|V_{i,+}|^2} \right) \tag{33}$$

Two scenarios are adopted to analyze the performance of the SOPs-based operation strategy for unbalanced ADNs.

Scenario I: The initial operation state of unbalanced ADNs without SOPs is obtained.

Scenario II: The unbalanced optimal operation is conducted based on SOPs.

The optimization results are listed in Table III.

Table III shows that compared with Scenario I, the active power losses and the overall voltage unbalanced conditions $\lambda_{\mathrm{UI,sys}}$ in Scenario II are reduced by 65.98% and 66.67% due to the regulation of SOPs. The three-phase currents of the distribution substation outlet are also effectively balanced.

The three-phase operation strategies of SOPs in Scenario II are presented in Fig. 3.

Fig. 4 and Fig. 5 show the individual voltage unbalanced condition and voltage profile at all nodes for Scenario I and II. In contrast to Scenario I, the SOPs-based unbalanced operation strategy is implemented in Scenario II, which significantly mitigates the voltage unbalanced condition and improves the voltage profile.

B. Modified IEEE 123-Node System

The modified IEEE 123-node distribution system is adopted to verify the scalability of the proposed method on large-scale

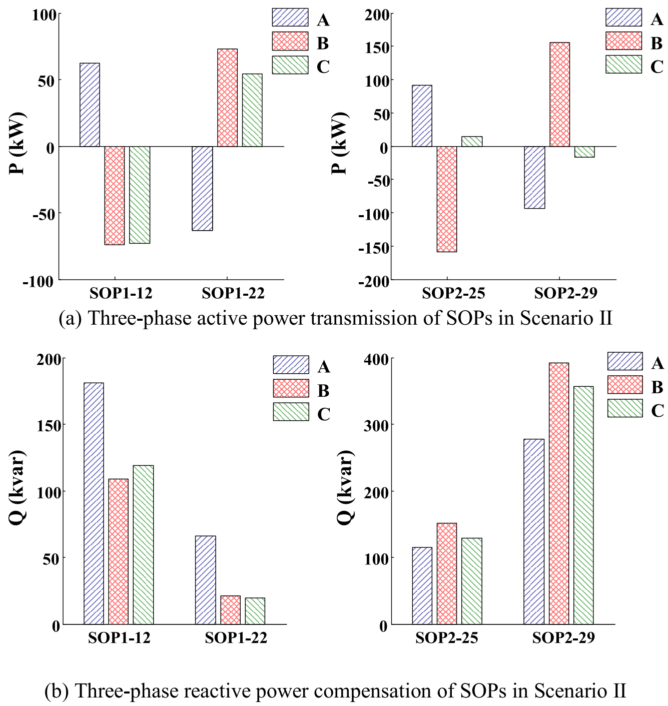

(a) Three-phase active power transmission of SOPs in Scenario II

(b) Three-phase reactive power compensation of SOPs in Scenario II

Fig. 3. Operation strategies of SOPs in Scenario II.

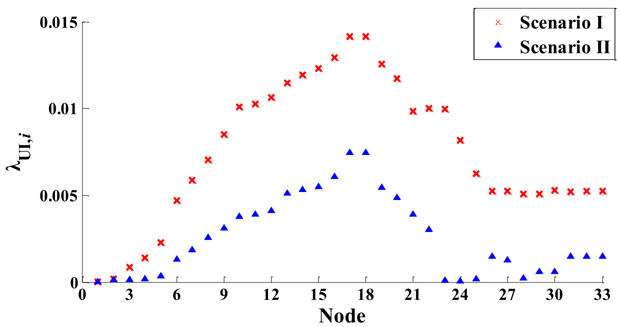

Fig. 4. Voltage unbalanced conditions for all nodes.

ADNs with severe unbalanced conditions, presented in Fig. 6. The rated voltage level is 4.16 kV. The total active and reactive power loads on the system are 3,490 kW and 1,920 kvar.

The system operates in a serious unbalanced condition. There are a number of branches with asymmetric parameters, single- and three-phase loads. The maximum load difference among the three phases is up to tens of kilowatts. The detailed parameters are provided in [48].

To fully consider the impact of asymmetric access of DGs with high penetration on ADNs, ten single-phase PVs are integrated into the network, and are operated with a constant power factor 1.0. The parameters are shown in Table IV. Two groups of SOP are installed between nodes 55 and 93, and between nodes 117 and 123, of which the parameters are same with those in Section IV-A.

C. Optimization Results Analysis

Considering the asymmetric access of DGs with high penetration, the SOP-based operation strategy can mitigate the three-phase unbalanced condition while minimizing the power losses of ADNs. Four scenarios are adopted to compare and analyze the performance of the operation strategy for unbalanced ADNs based on SOPs.

Scenario I: No PV integration in the system, the initial operation state of unbalanced ADNs without SOPs is obtained.

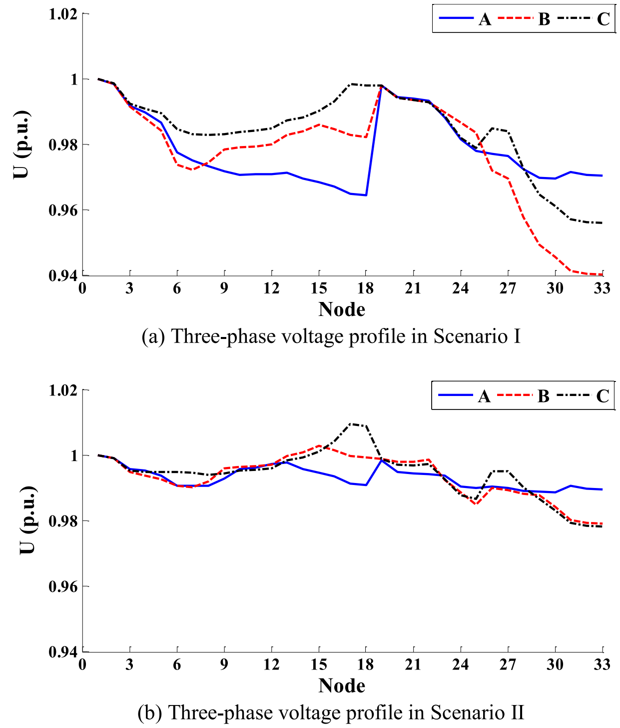

(a) Three-phase voltage profile in Scenario I

(b) Three-phase voltage profile in Scenario II

Fig. 5. Three-phase voltage profile in Scenario I and II.

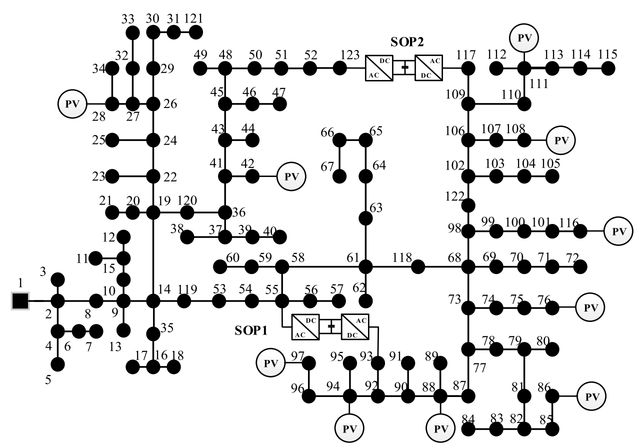

Fig. 6. Structure of the modified IEEE 123-node system.

TABLE IV
BASIC INSTALLATION PARAMETERS OF DGS

Parameter	PV cells									
Location	28	42	76	86	88	94	97	108	111	116
Phase	A	C	C	C	B	B	B	B	A	C
Capacity (kVA)	200	200	300	150	300	150	300	150	150	200

TABLE V
OPTIMIZATION RESULTS OF FOUR SCENARIOS

Scenario	Power losses (kW)	Reduction rate of losses (%)	$\lambda_{\mathrm{UI,sys}}$	Reduction rate of $\lambda_{\mathrm{UI,sys}}$ (%)	Three-phase current of substation outlet (A)
I	128.29	-	0.0094	-	747.74/448.87/580.82
II	93.84	26.85	0.0008	91.49	625.24/625.24/625.24
III	90.94	-	0.0136	-	689.47/291.55/355.76
IV	67.29	26.01	0.0012	91.18	561.59/561.59/561.59

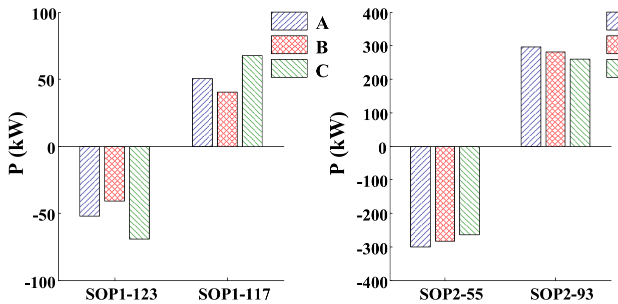

(a) Three-phase active power transmission of SOPs in Scenario II

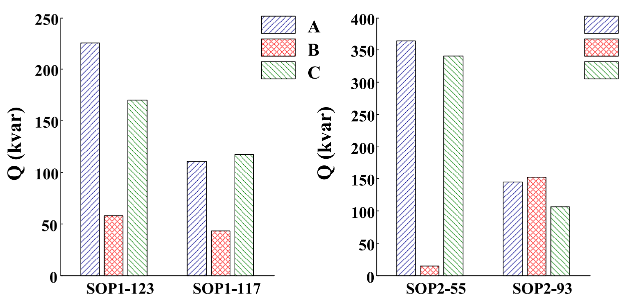

(b) Three-phase reactive power compensation of SOPs in Scenario II

Fig. 7. Operation Strategies of SOPs in Scenario II.

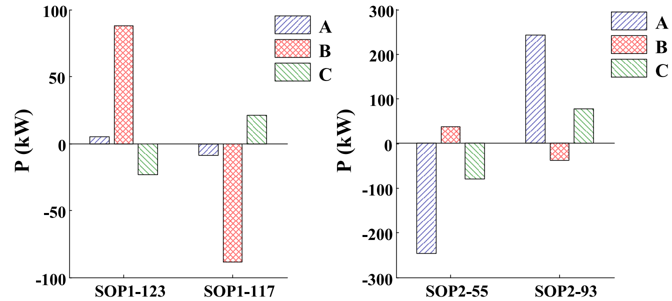

(a) Three-phase active power transmission of SOPs in Scenario IV

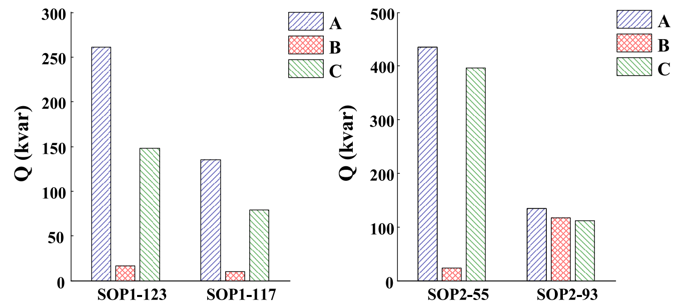

(b) Three-phase reactive power compensation of SOPs in scenario IV

Fig. 8. Operation strategies of SOPs in Scenario IV.

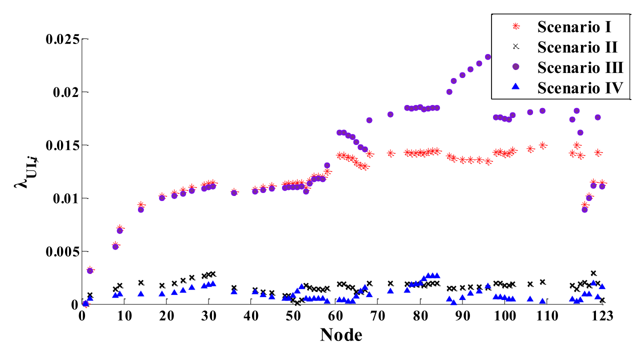

Fig. 9. Voltage unbalanced conditions for all nodes.

Scenario II: No PV integration in the system, the unbalanced optimal operation is conducted based on SOPs.

Scenario III: Considering 60% penetration of PVs, the initial state of unbalanced ADNs without SOPs is obtained.

Scenario IV: Considering 60% penetration of PVs, the unbalanced optimal operation is conducted based on SOPs.

The optimization results are listed in Table V.

Table V shows that compared with Scenario I, the unbalanced condition is exacerbated due to the 60% penetration of PVs in Scenario III. By regulating the operation of SOPs in Scenario II and Scenario IV, the active power losses are reduced by 26.85% and 26.01%, respectively. The overall voltage unbalanced conditions $\lambda_{\mathrm{UI,sys}}$ are reduced by 91.49% and 91.18%, which is a considerable improvement. The three-phase currents of the distribution substation outlet are also effectively balanced.

The three-phase operation strategies of SOPs in Scenario II and Scenario IV are presented in Fig. 7 and Fig. 8, respectively. It can be seen that in addition to the three-phase active power adjustment of SOPs, SOPs provide significant reactive power support, which can alleviate the three-phase reactive power demands of connected feeders and improve the voltage profile. As SOPs are based on B2B VSCs, the two converters can supply the reactive power compensation within their own capacity constraints. The three-phase reactive power outputs of SOPs locally compensate the reactive power demands, avoiding the remote transmission of reactive power from sources. Thus, the reactive power support of SOPs can effectively reduce power losses and improve the voltage profile.

Fig. 9 shows the individual voltage unbalanced condition at all nodes for four scenarios. In contrast to the other two scenarios, the proposed unbalanced operation strategy is implemented in Scenario II and Scenario IV, which reduces the negative sequence voltage of the system and significantly mitigates the node voltage unbalanced condition.

Regulating the operation of SOPs in ADNs can reduce power losses, mitigate three-phase unbalanced condition, and effectively mitigate each phase voltage deviation from the nominal value to improve the voltage profile. The results,

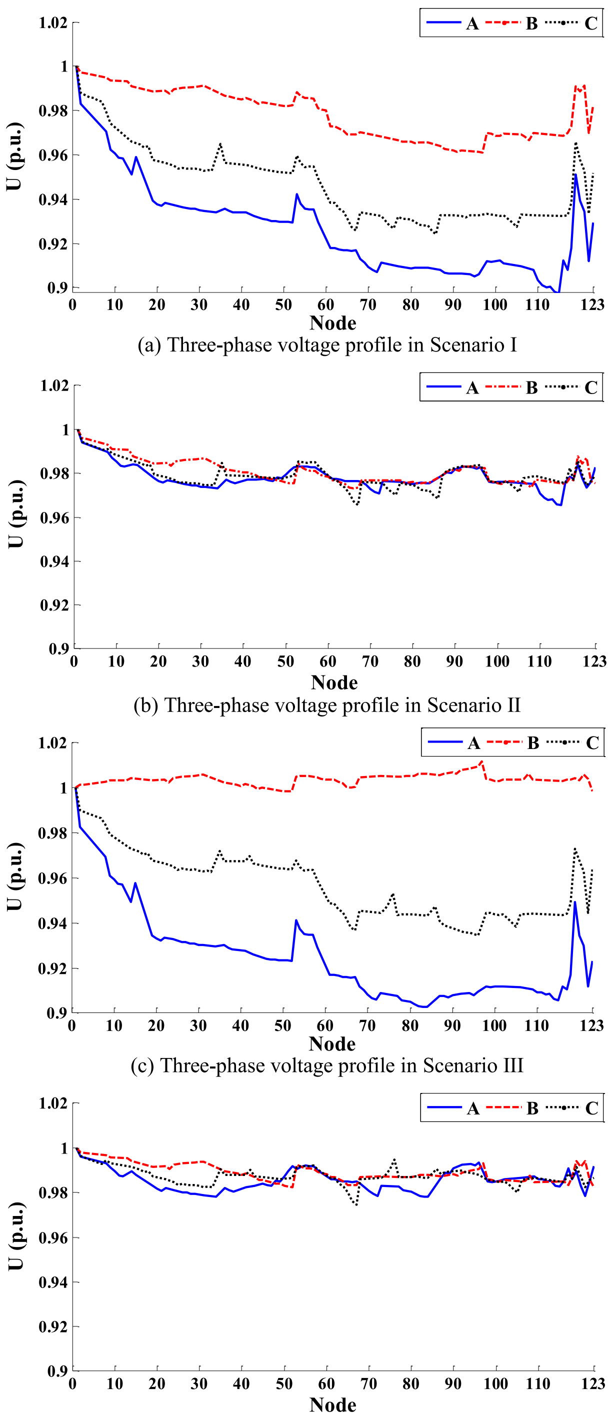

(a) Three-phase voltage profile in Scenario I

(b) Three-phase voltage profile in Scenario II

(c) Three-phase voltage profile in Scenario III

(d) Three-phase voltage profile in Scenario IV

Fig. 10. Three-phase voltage profile under different scenarios.

presented in Fig. 10, indicate that a relatively flat and tight voltage profile has been attained by SOP-based operation strategy.

To further demonstrate the benefits of SOPs, a comparison of the proposed strategy in Scenario IV and the solution of using energy storage systems (ESSs) is provided. And the SOPs-based three-phase optimization model has been extended to the time-series formulation to consider the power output fluctuation of DGs and the continuous adjustment of SOPs.

TABLE VI
COMPARISON OF THE TIME-SERIES RESULTS FOR SCENARIO IV AND V

Scenario	Energy losses (kWh)	Reduction rate of losses (%)	$\lambda_{\mathrm{UI,sys}}$	Reduction rate of $\lambda_{\mathrm{UI,sys}}$ (%)
IV	543.10	45.40	0.0011	99.05
V	610.74	38.60	0.0162	85.84

Scenario V adopts the ESS-based solution [46] which has the same operation objective (8).

Scenario V: Considering 60% penetration of PVs, the regulating of unbalanced operation is based on ESSs.

In Scenario V, two ESSs with the converter capacity of 500 kVA on each phase are connected to nodes 52 and 55 respectively, and each ESS has the same converter capacity as the SOP. The maximum energy reservoir capacity of the ESS is 1,000 kWh. The locations and capacities of ESSs are referenced as the configuration of the SOPs in Scenario IV.

The three phases power of ESSs are controlled independently, assuming the ESSs consist of three single-phase ESS modules [20]. As the energy stored in ESSs is time varying, the additional storage dynamics and operation constraints of ESSs [46] are shown as follows.

$$E^{\mathrm{ESS}}_{\varphi,i,t+1} = E^{\mathrm{ESS}}_{\varphi,i,t} - \left(P^{\mathrm{ESS}}_{\varphi,i,t} + P^{\mathrm{ESS,l}}_{\varphi,i,t}\right)\Delta t \tag{34}$$

$$\underline{E}^{\mathrm{ESS}}_{\varphi,i} \le E^{\mathrm{ESS}}_{\varphi,i,t} \le \overline{E}^{\mathrm{ESS}}_{\varphi,i} \tag{35}$$

$$E^{\mathrm{ESS}}_{\varphi,i,N_{\mathrm{T}}} = E^{\mathrm{ESS}}_{\varphi,i,0} \tag{36}$$

$$P^{\mathrm{ESS,l}}_{\varphi,i,t} = A^{\mathrm{ESS}}_{i}\sqrt{\left(P^{\mathrm{ESS}}_{\varphi,i,t}\right)^2 + \left(Q^{\mathrm{ESS}}_{\varphi,i,t}\right)^2} \tag{37}$$

$$\sqrt{\left(P^{\mathrm{ESS}}_{\varphi,i,t}\right)^2 + \left(Q^{\mathrm{ESS}}_{\varphi,i,t}\right)^2} \le S^{\mathrm{ESS}}_{\varphi,i} \tag{38}$$

where $E^{\mathrm{ESS}}_{\varphi,i,t}$ denotes the stored energy of ESSs. $P^{\mathrm{ESS}}_{\varphi,i,t}$ denotes the injected/extracted power and $P^{\mathrm{ESS,l}}_{\varphi,i,t}$ denotes the power losses of ESSs. It is assumed that injecting power from ESSs into networks is the positive direction.

Constraint (34) determines that the stored energy of ESSs at time $(t+1)$ depends on the previous state of charge and the injected/extracted power of the time interval. Constraint (35) limits stored energy within the desired level, i.e., from 20% to 100%. Constraint (36) imposes that the initial state of charge and final state of charge are kept consistent during the time horizon N_{T} of optimization.

As (34)-(36) are all linear constraints and (37)-(38) can be similarly reformulated as SDP constraints, the proposed SDP model can also be applied to solve the ESSs-based solution with the same optimization objective (8) in Scenario V.

The daily PVs and loads operation profiles are obtained from [49]. The time-series optimization results comparing Scenario IV and V are listed in Table VI. The results of time-series simulation are shown in Fig. 11 and Fig. 12.

ESSs can effectively realize the temporal power regulation by charging or discharging, while SOPs accomplish the spatial power transformation by flexible connecting adjacent feeders. Table VI indicates that the improvements of energy loss reduction and unbalanced conditions mitigation in Scenario IV are

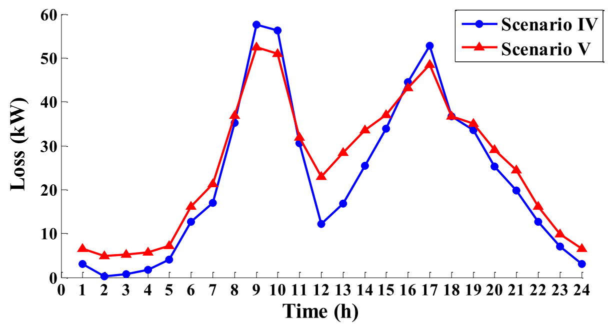

Fig. 11. Comparison of the active power losses in Scenario IV and V.

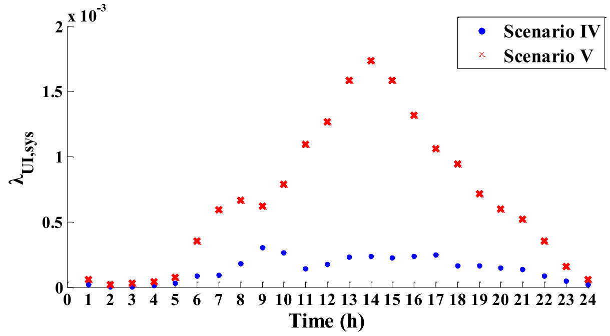

Fig. 12. Comparison of the system UI in Scenario IV and V.

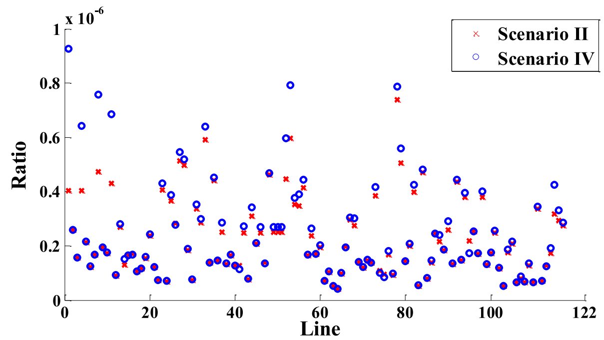

Fig. 13. Verification of SDP relaxation accuracy.

more significant than that in Scenario V. It should be noted that the effect and flexibilities sourced from SOPs and ESSs may vary with the system configuration and conditions, among which a key factor is the system load level.

As shown from the above analysis, the proposed strategy regulates the operation of SOPs to optimize the three-phase active and reactive power flow of whole system. It alleviates the unbalanced condition and decreases the operational losses, ensuring a secure and economic operation of ADNs.

D. Algorithm Validation

As defined in Section III-C, the ratio value indicates the ratio of largest two eigenvalues of the matrix in (15), which is used to evaluate the exactness of SDP relaxation. The maximum ratio value for each line in the above studied cases is shown in Fig. 13, and it satisfies that the ratios are smaller than 1.0e-6 over all lines. Thus, the SDP relaxation is numerically exact for the studied cases.

TABLE VII
PERFORMANCE COMPARISON OF PROPOSED STRATEGY AND IPM

Scenario	Power losses (MW)		$\lambda_{\mathrm{UI,sys}}$ (p.u.)		Time (s)	
	IPM	Proposed strategy	IPM	Proposed strategy	IPM	Proposed strategy
I	0.12827	0.12829	6.4102	6.4102	10.93	1.74
II	0.09381	0.09384	0.4893	0.4896	13.63	1.45
III	0.09092	0.09094	10.0987	10.0987	11.57	1.62
IV	0.06728	0.06729	0.6579	0.6581	12.59	1.36

To verify the convergence and efficiency of the proposed strategy based on SDP, IPOPT [50] in the GAMS software is used to solve the initial NLP model comprising (23) with the same parameters as those of the abovementioned scenarios in IEEE 123-node distribution system. IPOPT is an optimization package based on the IPM, which can obtain the high quality optimum and has been widely applied in solving the NLP problem. A performance comparison is shown in Table VII.

Table VII shows that compared with the IPM used in IPOPT, the proposed SDP-based strategy promotes the computing speed while solving the unbalanced operation optimization problem accurately for the studied cases. Because of the convex relaxation to the original problem, the adopted SDP model shows improved computational efficiency by ensuring convexity and reducing the computational complexity of the problem. The improvement will facilitate online application of the proposed strategy.

V. CONCLUSION

This paper presents an operation strategy based on SOPs to minimize the operational losses and mitigate three-phase unbalances in ADNs. Considering the asymmetric access of high penetration levels of DGs, an operation optimization model for unbalanced ADNs is developed based on SOPs. The optimization results indicate that the SOPs-based strategy significantly mitigates the unbalanced condition and reduces the power losses in ADNs. The original NLP model is converted into an SDP model via convex relaxation. The numerical tests empirically show that the proposed SDP relaxation model is numerically exact with improved computational efficiency for the studied cases, which makes it suitable for solving the unbalanced optimization of large-scale ADNs with high penetration levels of DGs.

Taking into account the relatively high investment of SOPs and the coordination with conventional regulation devices, such as on-load tap changer (OLTC) and tie switches, an extension of the coordinated operation strategy will be more practical for the realistic operation of ADNs and needs to be fully considered. For three-phase adjustment of devices with discrete variables, a more efficient operation strategy based on mixed-integer SDP for unbalanced ADNs also warrants further research.

References

[1] A. C. Rueda-Medina and A. Padilha-Feltrin, "Distributed generators as providers of reactive power support—A market approach," *IEEE Trans. Power Syst.*, vol. 28, no. 1, pp. 490–502, Feb. 2013.

[2] P. Hallberg *et al.*, "Active distribution system management a key tool for the smooth integration of distributed generation," *Eurelectric TF Active System Management*, 2013.

[3] K. Kuroda, H. Magori, T. Ichimura, and R. Yokoyama, "A hybrid multi-objective optimization method considering optimization problems in power distribution systems," *J. Mod. Power Syst. Clean Energy*, vol. 3, no. 1, pp. 41–50, 2015.

[4] H. Ye, J. Wang, Y. Ge, J. Li, and Z. Li, "Robust integration of high-level dispatchable renewables in power system operation," *IEEE Trans. Sustain. Energy*, vol. 8, no. 2, pp. 826–835, Apr. 2017.

[5] M. Tan, C. Han, X. Zhang, L. Guo, and T. Yu, "Hierarchically correlated equilibrium Q-learning for multi-area decentralized collaborative reactive power optimization," *CSEE J. Power Energy Syst.*, vol. 2, no. 3, pp. 65–72, Sep. 2016.

[6] S. Bruno, S. Lamonaca, G. Rotondo, U. Stecchi, and M. La Scala, "Unbalanced three-phase optimal power flow for smart grids," *IEEE Trans. Ind. Electron.*, vol. 58, no. 10, pp. 4504–4513, Oct. 2011.

[7] E. Carpaneto, G. Chicco, and J. S. Akilimali, "Loss partitioning and loss allocation in three-phase radial distribution systems with distributed generation," *IEEE Trans. Power Syst.*, vol. 23, no. 3, pp. 1039–1049, Aug. 2008.

[8] K. Ma, R. Li, and F. Li, "Quantification of additional asset reinforcement cost from 3-phase imbalance," *IEEE Trans. Power Syst.*, vol. 31, no. 4, pp. 2885–2891, Jul. 2016.

[9] K. Ma, F. Li, and R. Aggarwal, "Quantification of additional reinforcement cost driven by voltage constraint under three-phase imbalance," *IEEE Trans. Power Syst.*, vol. 31, no. 6, pp. 5126–5134, Nov. 2016.

[10] P. D. F. Ferreira, P. M. S. Carvalho, L. A. F. M. Ferreira, and M. D. Ilic, "Distributed energy resources integration challenges in low-voltage networks: Voltage control limitations and risk of cascading," *IEEE Trans. Sustain. Energy*, vol. 4, no. 1, pp. 82–88, Jan. 2013.

[11] M. W. Siti, D. V. Nicolae, A. A. Jimoh, and A. Ukil, "Reconfiguration and load balancing in the LV and MV distribution networks for optimal performance," *IEEE Trans. Power Del.*, vol. 22, no. 4, pp. 2534–2540, Oct. 2007.

[12] R. A. Hooshmand and S. Soltani, "Fuzzy optimal phase balancing of radial and meshed distribution networks using BF-PSO algorithm," *IEEE Trans. Power Syst.*, vol. 27, no. 1, pp. 47–57, Feb. 2012.

[13] M. B. Liu, C. A. Canizares, and W. Huang, "Reactive power and voltage control in distribution systems with limited switching operations," *IEEE Trans. Power Syst.*, vol. 24, no. 2, pp. 889–899, May 2009.

[14] J. M. Bloemink and T. C. Green, "Increasing distributed generation penetration using soft normally-open points," in *Proc. IEEE Power Energy Soc. Gen. Meeting*, Providence, RI, USA, 2010, pp. 1–8.

[15] W. Cao, J. Wu, N. Jenkins, C. Wang, and T. Green, "Operating principle of soft open points for electrical distribution network operation," *Appl. Energy*, vol. 164, pp. 245–257, Feb. 2016.

[16] N. Daratha, B. Das, and J. Sharma, "Coordination between OLTC and SVC for voltage regulation in unbalanced distribution system distributed generation," *IEEE Trans. Power Syst.*, vol. 29, no. 1, pp. 289–299, Jan. 2014.

[17] H. A. Mostafa, R. El-Shatshat, and M. M. A. Salama, "Multi-objective optimization for the operation of an electric distribution system with a large number of single phase solar generators," *IEEE Trans. Smart Grid*, vol. 4, no. 2, pp. 1038–1047, Jun. 2013.

[18] Z. Tian, W. Wu, B. Zhang, and A. Bose, "Mixed-integer second-order cone programing model for VAR optimisation and network reconfiguration in active distribution networks," *IET Gener. Transm. Distrib.*, vol. 10, no. 8, pp. 1938–1946, May 2016.

[19] B. A. Robbins and A. D. Dominguez-Garcia, "Optimal reactive power dispatch for voltage regulation in unbalanced distribution systems," *IEEE Trans. Power Syst.*, vol. 31, no. 4, pp. 2903–2913, Jul. 2016.

[20] Z. Wang, J. Wang, and C. Chen, "A three-phase microgrid restoration model considering unbalanced operation of distributed generation," *IEEE Trans. Smart Grid*, to be published.

[21] X. Bai, H. Wei, K. Fujisawa, and Y. Wang, "Semidefinite programming for optimal power flow problems," *Int. J. Elect. Power Energy Syst.*, vol. 30, nos. 6–7, pp. 383–392, 2008.

[22] B. A. Robbins, H. Zhu, and A. D. Domínguez-García, "Optimal tap setting of voltage regulation transformers in unbalanced distribution systems," *IEEE Trans. Power Syst.*, vol. 31, no. 1, pp. 256–267, Jan. 2016.

[23] E. Dall'Anese, H. Zhu, and G. B. Giannakis, "Distributed optimal power flow for smart microgrids," *IEEE Trans. Smart Grid*, vol. 4, no. 3, pp. 1464–1475, Sep. 2013.

[24] E. Dall'Anese, S. V. Dhople, and G. B. Giannakis, "Optimal dispatch of photovoltaic inverters in residential distribution systems," *IEEE Trans. Sustain. Energy*, vol. 5, no. 2, pp. 487–497, Apr. 2014.

[25] W. Cao, J. Wu, N. Jenkins, C. Wang, and T. Green, "Benefits analysis of soft open points for electrical distribution network operation," *Appl. Energy*, vol. 165, pp. 36–47, Mar. 2016.

[26] C. Long, J. Wu, L. Thomas, and N. Jenkins, "Optimal operation of soft open points in medium voltage electrical distribution networks with distributed generation," *Appl. Energy*, vol. 184, pp. 427–437, Dec. 2016.

[27] K. Lehmann, A. Grastien, and P. Van Hentenryck, "AC-feasibility on tree networks is NP-hard," *IEEE Trans. Power Syst.*, vol. 31, no. 1, pp. 798–801, Jan. 2016.

[28] S. H. Low, "Convex relaxation of optimal power flow—Part I: Formulations and equivalence," *IEEE Trans. Control Netw. Syst.*, vol. 1, no. 1, pp. 15–27, Mar. 2014.

[29] S. H. Low, "Convex relaxation of optimal power flow—Part II: Exactness," *IEEE Trans. Control Netw. Syst.*, vol. 1, no. 2, pp. 177–189, Jun. 2014.

[30] J. M. Bloemink and T. C. Green, "Benefits of distribution-level power electronics for supporting distributed generation growth," *IEEE Trans. Power Del.*, vol. 28, no. 2, pp. 911–919, Apr. 2013.

[31] L. R. Araujo, D. R. R. Penido, S. Carneiro, and J. L. R. Pereira, "A three-phase optimal power-flow algorithm to mitigate voltage unbalance," *IEEE Trans. Power Del.*, vol. 28, no. 4, pp. 2394–2402, Oct. 2013.

[32] A. M. Jubril, O. A. Komolafe, and K. O. Alawode, "Solving multi-objective economic dispatch problem via semidefinite programming," *IEEE Trans. Power Syst.*, vol. 28, no. 3, pp. 2056–2064, Aug. 2013.

[33] T. L. Saaty, "Decision making—The analytic hierarchy and network processes (AHP/ANP)," *J. Syst. Sci. Syst. Eng.*, vol. 13, no. 1, pp. 1–35, 2004.

[34] M. E. Baran and F. F. Wu, "Optimal capacitor placement on radial distribution systems," *IEEE Trans. Power Del.*, vol. 4, no. 1, pp. 725–734, Jan. 1989.

[35] L. Gan and S. H. Low, "Convex relaxations and linear approximation for optimal power flow in multiphase radial networks," in *Proc. 18th IEEE Power Syst. Comput. Conf. (PSCC)*, Wrocław, Poland, 2014, pp. 1–9.

[36] Q. Peng, "Distributed control and optimization for communication and power systems," Ph.D. dissertation, Dept. Elect. Eng., California Inst. Technol., Pasadena, CA, USA, 2016.

[37] H. Wolkowitz, R. Saigal, and L. Vandenberghe, *Handbook of Semidefinite Programming: Theory, Algorithms and Applications*. Boston, MA, USA: Kluwer Acad., 2000.

[38] D. M. W. Leenaerts and W. M. G. van Bokhoven, *Piecewise Linear Modelling and Analysis*. Dordrecht, The Netherlands: Kluwer Acad., 1998.

[39] M. S. Lobo, L. Vandenberghe, S. Boyd, and H. Lebret, "Applications of second-order cone programming," *Linear Algebra Appl.*, vol. 284, nos. 1–3, pp. 193–228, 1998.

[40] Z.-Q. Luo, W.-K. Ma, A. M.-C. So, Y. Ye, and S. Zhang, "Semidefinite relaxation of quadratic optimization problems," *IEEE Signal Process. Mag.*, vol. 27, no. 3, pp. 20–34, May 2010.

[41] C. Coffrin, H. Hijazi, and P. van Hentenryck, "Strengthening the SDP relaxation of AC power flows with convex envelopes, bound tightening, and valid inequalities," *IEEE Trans. Power Syst.*, vol. 32, no. 5, pp. 3549–3558, Sep. 2017.

[42] B. Kocuk, S. S. Dey, and X. A. Sun, "Inexactness of SDP relaxation and valid inequalities for optimal power flow," *IEEE Trans. Power Syst.*, vol. 31, no. 1, pp. 642–651, Jan. 2016.

[43] J. Lavaei and S. H. Low, "Zero duality gap in optimal power flow problem," *IEEE Trans. Power Syst.*, vol. 27, no. 1, pp. 92–107, Feb. 2012.

[44] L. Gan, N. Li, U. Topcu, and S. H. Low, "Exact convex relaxation of optimal power flow in radial networks," *IEEE Trans. Autom. Control*, vol. 60, no. 1, pp. 72–87, Jan. 2015.

[45] J. Lofberg, "YALMIP: A toolbox for modeling and optimization in MATLAB," in *Proc. CASCD Conf.*, New Orleans, LA, USA, 2004, pp. 284–289.

[46] M. Nick, R. Cherkaoui, and M. Paolone, "Optimal allocation of dispersed energy storage systems in active distribution networks for energy balance and grid support," *IEEE Trans. Power Syst.*, vol. 29, no. 5, pp. 2300–2310, Sep. 2014.

[47] M. J. E. Alam, K. M. Muttaqi, and D. Sutanto, "A three-phase power flow approach for integrated 3-wire MV and 4-wire multigrounded LV networks with rooftop solar PV," *IEEE Trans. Power Syst.*, vol. 28, no. 2, pp. 1728–1737, May 2013.

[48] W. H. Kersting, "Radial distribution test feeders," *IEEE Trans. Power Syst.*, vol. 6, no. 3, pp. 975–985, Aug. 1991.

[49] P. Li *et al.*, "A coordinated control method of voltage and reactive power for active distribution networks based on soft open point," *IEEE Trans. Sustain. Energy*, to be published.

[50] A. Wächter and L. T. Biegler, "On the implementation of an interior-point filter line-search algorithm for large-scale nonlinear programming," *Math. Program.*, vol. 106, no. 1, pp. 25–57, 2006.

Peng Li (M'11) received the B.S. and Ph.D. degrees in electrical engineering from Tianjin University, Tianjin, China, in 2004 and 2010, respectively.

He is currently an Associate Professor with the School of Electrical and Information Engineering, Tianjin University. His current research interests include distributed generation system and microgrid, smart distribution system, and transient simulation and analysis.

Haoran Ji (S'16) received the B.S. degree in electrical engineering from Tianjin University, Tianjin, China, in 2014, where he is currently pursuing the Ph.D. degree in electrical engineering.

His current research interests include distribution system modeling and optimization.

Chengshan Wang (SM'11) received the Ph.D. degree in electrical engineering from Tianjin University, Tianjin, China, in 1991.

From 1994 to 1996, he was a Senior Academic Visitor with Cornell University, Ithaca, NY, USA. From 2001 to 2002, he was a Visiting Professor with Carnegie Mellon University, Pittsburgh, PA, USA. He is currently a Professor with the School of Electrical and Information Engineering, Tianjin University, where he is the Director of the Key Laboratory of Smart Grid of Ministry of Education. His current research interests include distribution system analysis and planning, distributed generation system and microgrid, and power system security analysis.

Prof. Wang is an Editorial Board Member of *Applied Energy*, and the *Journal of Modern Power Systems and Clean Energy*.

Jinli Zhao (M'11) received the Ph.D. degree in electrical engineering from Tianjin University, Tianjin, China, in 2007.

She is currently an Associate Professor with the School of Electrical and Information Engineering, Tianjin University. Her research focuses on power system security and stability.

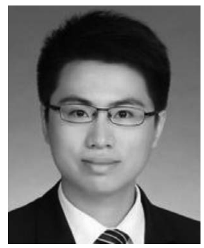

Guanyu Song received the B.S. and Ph.D. degrees in electrical engineering from Tianjin University, Tianjin, China, in 2012 and 2017, respectively.

He is currently a Lecturer with the School of Electrical and Information Engineering, Tianjin University. His current research interests include optimal planning and operation of smart distribution system.

Fei Ding (M'14) received the Ph.D. degree from Case Western Reserve University. She joined National Renewable Energy Laboratory as a Research Engineer in 2015.

Her research focuses on distribution system automation and optimization, distribution system modeling and simulation, renewable energy grid integration, microgrid and smart grid.

Jianzhong Wu (M'14) received the Ph.D. degree from Tianjin University, Tianjin, China, in 2004.

From 2004 to 2006, he was with Tianjin University, where he is an Associate Professor. From 2006 to 2008, he was a Research Fellow with the University of Manchester, Manchester, U.K. He is currently a Professor with the Cardiff School of Engineering, Institute of Energy, London, U.K. His current research interests include energy infrastructure and smart grids.

Dr. Wu is a member of the Institution of Engineering and Technology and the Association for Computing Machinery.